JACS
JOURNAL OF THE AMERICAN CHEMICAL SOCIETY

ARTICLE

pubs.acs.org/JACS

Observation of a Single-Stranded DNA/Pyrrolobenzodiazepine Adduct

Khondaker M. Rahman,[†] Colin H. James,[†] Tam T. T. Bui,[‡] Alex F. Drake,[‡] and David E. Thurston*[,†,§]

[†]Gene Targeted Drug Design Research Group, The School of Pharmacy, University of London, 29/39 Brunswick Square, London WC1N 1AX, U.K.

[‡]Biomolecular Spectroscopy Centre, Kings College London, Guy's Campus, London SE1 1UL, U.K.

[§]Spirogen Ltd., The School of Pharmacy, University of London, London WC1N 1AX, U.K.

Supporting Information

ABSTRACT: Pyrrolobenzodiazepine (PBD) antitumor agents have, to date, only been observed to bind to duplex DNA, apparently requiring a minor groove environment for covalent bond formation between their C11-position and the C2-NH_2 functionality of a guanine base. Using an HPLC/MS assay we have now observed and isolated for the first time PBD adducts with single-stranded DNA fragments. Surprisingly, these adducts could only be formed through dissociation of duplex DNA adducts and not by direct interaction of PBDs with single-stranded DNA. They were sufficiently stable for characterization by MALDI-TOF-MS and remained intact after storing at −20 °C for at least 20 days, although the PBD became detached from the DNA within 7 days if stored at room temperature. Furthermore, addition of a complementary strand allowed the duplex adduct to reform. The relative stability of single-stranded PBD/DNA adducts despite a complete loss of minor groove structure was further confirmed by CD spectroscopic analysis. The CD signal induced by the presence of a PBD molecule in the single-stranded adducts remained prominent despite heating for 2 h at 50−60 °C, thus indicating their relatively robust nature.

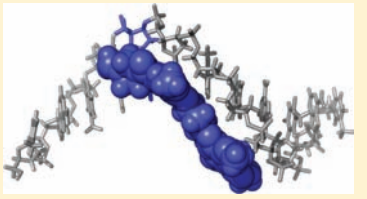

INTRODUCTION

The pyrrolo[2,1-*c*][1,4]benzodiazepines (PBDs) are sequence-selective DNA minor-groove binding agents.[1−5] The naturally occurring PBDs produced by *Streptomyces* and *Micrococcus* species are monomeric (*e.g.*, anthramycin **1**, Figure 1A) and form singly alkylated DNA adducts, whereas the synthetic PBD dimers (*e.g.*, SJG-136,[6] **2**; DRG-16,[7] **3**; Figure 1A) consist of two PBD units joined through a C8/C8′-linker and can form interstrand or intrastrand DNA cross-links in addition to monoadducts.[8] One PBD dimer (SJG-136, **2**) has successfully completed phase I clinical trials[9−11] and is presently undergoing phase II evaluation in ovarian and hematological cancers. PBDs have a chiral center at their C11a(*S*)-position which provides them with an appropriate three-dimensional (3D) shape to fit securely within the DNA minor groove.[4] In addition, they possess an electrophilic N10−C11 moiety (*i.e.*, interconvertible imine, carbinolamine, or carbinolamine methyl ether functionalities) that can form a covalent aminal linkage between their C11-position and the nucleophilic C2-NH_2 group of a guanine base (Figure 1B).[4] PBD monomers such as anthramycin (**1**) typically span three base pairs of DNA with a reported preference for 5′-Pu-G-Pu-3′ sequences,[4,12] although more recent data suggest that they have a kinetic preference for 5′-Py-G-Py-3′ sequences.[13] On the other hand, synthetic PBD dimers such as SJG-136 (**2**) and DRG-16 (**3**) (Figure 1A) can span six or more base pairs, depending on the length of the linker connecting the monomeric units.[1,7] In addition to the PBD dimers, a range of synthetic monomeric PBDs of extended length has been developed by linking noncovalent minor-groove binding components to the C8-position of the PBD A ring[14−20] (*e.g.*, GWL-78,[19] **4**). It is known from the literature that monomeric PBDs can stabilize duplex DNA through formation of covalent adducts.[4,19,20] PBD dimers, which form inter- and intrastrand cross-linked adducts, can stabilize DNA to an even greater extent.[6,7] For both PBD monomers and dimers, this stabilizing property has been shown to correlate well with their *in vitro* cytotoxicity.[6,7,19,21] PBDs have been shown to mediate a number of biological effects including the inhibition of endonucleases,[22] RNA polymerase,[19,22] and transcription factor binding.[20,24−26] They have also been shown to have antimicrobial activity.[27−30] Covalent PBD/DNA adducts have been studied by high-field NMR,[31−33] molecular modeling,[7,32,34,35] HPLC/MS,[8,36−40] mass spectrometry,[41] and biochemical methods[42] and have been used as pharmacodynamic biomarkers during the phase I clinical trials of SJG-136 (**1**).[9−11] The most likely basis for the selective biological activity of PBDs is preferential DNA repair in healthy cells, with the repair response to different cross-linking agents in tumor cells depending on cell type and the extent and duration of exposure to a particular agent.[43] Tumor cells are often deficient in one or more relevant DNA repair pathways, thus leading to selective cytotoxicity and an antitumor effect *in vivo*.[44] Thus, the ability of tumor cells to carry out DNA repair will, along with other factors,

Received: June 10, 2011
Published: September 19, 2011

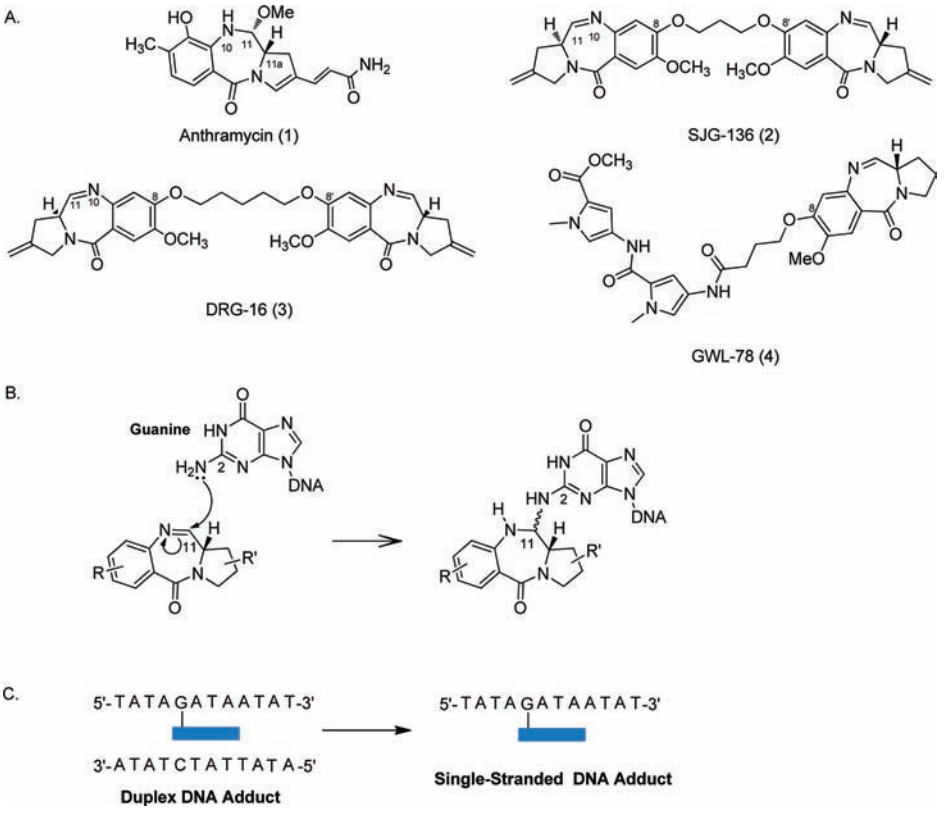

Figure 1. (A) Structures of the naturally occurring monomeric PBD anthramycin (**1**), the synthetic DNA cross-linking PBD dimers SJG-136 (**2**) and DRG-16 (**3**), and the C8-linked PBD-*bis*-pyrrole conjugate GWL-78 (**4**). (B) Mechanism for a monomeric PBD binding covalently through its C11-position to the C2-NH_2 of a guanine base. (C) Schematic diagram of a duplex monoadduct of a PBD dissociating to a stable single-stranded DNA adduct (PBD is depicted as a blue rectangle).

lead to the development of resistance which can influence both *in vitro* and *in vivo* efficacy.

It has been previously demonstrated that loss of minor-groove structure through denaturation of DNA can lead to detachment of up to 70% of bound ligand from PBD adduct-containing DNA.[45] In addition, we recently reported the dynamic nature of a hairpin DNA structure when covalently attached to a PBD molecule.[38] This study demonstrated the ability of a PBD molecule to remain attached to a hairpin DNA fragment despite a transient loss of minor-groove structure during structural transformation. A further recent study showed that PBD/DNA adducts are reversible and that, after heat-induced detachment from DNA, a PBD molecule can re-attach at room temperature.[37] These observations led us to the current investigation of whether PBDs can remain bonded to single-stranded DNA despite a complete and permanent loss of minor-groove structure. Using HPLC/MS and CD methodologies, we have now been able to observe stable single-stranded PBD adducts for both PBD monomer and dimer molecules (Figure 1C), capable of withstanding denaturing HPLC conditions and storage for between 72 to 168 h at room temperature and −20 °C, both in solution and in lyophilized form.

This observation is important in view of the ongoing phase II clinical trials of SJG-136 and the preclinical development of PBD/antibody conjugates, as there is growing interest in the precise mechanism of action of these agents. It is possible that stable single-stranded PBD adducts may form in cells through the action of repair and other types of enzymes that separate double-stranded DNA. Therefore, the observation reported here has implications for the mechanism of action of PBDs, the repair of adducts in cells and hence clinical resistance. It could also influence the choice of biomarker assay used in future clinical trials. For example, for PBD dimers, the γH2X foci assay[46] which detects more-generalized DNA damage may be more relevant than the COMET assay[47] which is used mainly to detect duplex interstrand cross-linked adducts.

RESULTS AND DISCUSSION

For this study we utilized PBD dimers SJG-136 (**2**) and DRG-16 (**3**) and the PBD monomer GWL-78 (**4**), along with the previously reported HPLC/MS analytical methodology[8,38,41] and the oligonucleotides listed in Table 1. The dimeric SJG-136 was chosen for the study as it is being investigated in human clinical trials at present;[9−11] thus, new data for this molecule could help with understanding its mechanism of action. DRG-16 was chosen to confirm that a PBD dimer with a longer central C8/C8′ linker could also form a single-stranded adduct, while GWL-78 was included to examine whether a PBD monomer would exhibit the same behavior, thus confirming the universality of this phenomenon for PBD molecules. Although PBD dimers have been shown to form intra- and intermolecular cross-links in addition to monoadducts[8] with double-stranded DNA, the oligonucleotide duplexes used in this study were designed to contain just one reactive guanine, thus allowing only monoalkylated adducts to form. Incubation of the three PBD molecules with these annealed oligonucleotide duplexes for specific time

Table 1. Oligonucleotides Used in the Study

label		DNA sequence
Seq-1/*Seq-1*	Duplex 1	5′-TATAGATCTATA-3′
		3′-ATATCTAGATAT-5′
*Seq-1*ino A	Duplex 2	5′-TATAGATITATA-3′
Seq-2		3′-ATATCTACATAT-5′
*Seq-1*ino B	Duplex 3	5′-TATAIATGTATA-3′
Seq-2		3′-ATATCTACATAT-5′
Seq-3	Duplex 4	5′-TATAGATAATAT-3′
Seq-4		3′-ATATCTATTATA-5′
Seq-5	Duplex 5	5′-TATATATGTTAT-3′
Seq-6		3′-ATATATACAATA-5′
Seq-7	Duplex 6	5′-TATAGATAT-3′
Seq-8		3′-ATATCTATA-5′
Seq-9	Duplex 7	5′-TATAGATAATTAATAT-3′
Seq-10		3′-ATATCTATTAATTATA-5′
Seq-11		5′-ATATGATCTATA-3′

periods followed by injection of the reaction mixtures onto the HPLC column provided distinct adduct peaks that could be collected, lyophilized, and subjected to MALDI-TOF-MS to confirm their identity. Unreacted single-stranded oligonucleotides and annealed duplexes were also analyzed in the same HPLC system to provide reference peaks. As with previously reported studies,[8,36] a 4:1 molar ratio of ligand/oligonucleotide was used, as this ensured completion of adduct formation within a reasonable time frame.

We initially confirmed the previously reported interstrand cross-link that can form between **2** and the Pu-GATC-Py sequence (Figure S1, Supporting Information [SI]) within the self-complementary 12-mer duplex oligonucleotide formed from *Seq-1* (Table 1). In order to obtain a monoalkylated adduct we designed a modified duplex (*Seq-1inoA*/*Seq-2*; Duplex 2, Table 1) in which only one reactive guanine was available for alkylation, with the other guanine mutated to a non-nucleophilic inosine base. Analysis of Duplex 2 alone using identical HPLC conditions, gave two peaks at RT 24.7 and 26.4 min (Figure 2A), identified by MALDI-TOF-MS as the denatured single-stranded *Seq-1inoA* and *Seq-2* species, respectively. This was consistent with our previous report that DS oligonucleotides of this length denature under these HPLC conditions.[8,41]

Incubating **2** with Duplex 2 for 6 h allowed completion of monoalkylation, and provided a new peak at RT 33.6 min with concomitant disappearance of the RT 24.7 min peak while the RT 26.4 min peak remained unaltered (Figure 2B). Further observations confirmed that while **2** must have initially formed a monoadduct with the *Seq-1inoA*/*Seq-2* duplex thus consuming both DNA species at an equal rate, on the HPLC column the duplex adduct dissociated into a **2**/*Seq1inoA* complex (33.6 min) and the free *Seq-2* strand (26.4 min), thus explaining the disappearance of the *Seq-1inoA* peak at RT 24.7 min. The 33.6 min peak was collected and subjected to MALDI-TOF-MS with the observed mass (m/z 4224, SI) corresponding to the 1:1 **2**/*Seq-1inoA* monoadduct. To assess the stability of this single-stranded adduct, after collection it was reinjected onto the HPLC column after 1 h. The resulting chromatogram (Figure 2C) showed an identical peak at RT 33.6 min, indicating that the single-stranded adduct was stable enough to withstand the HPLC conditions. This peak was collected again and its identity confirmed using

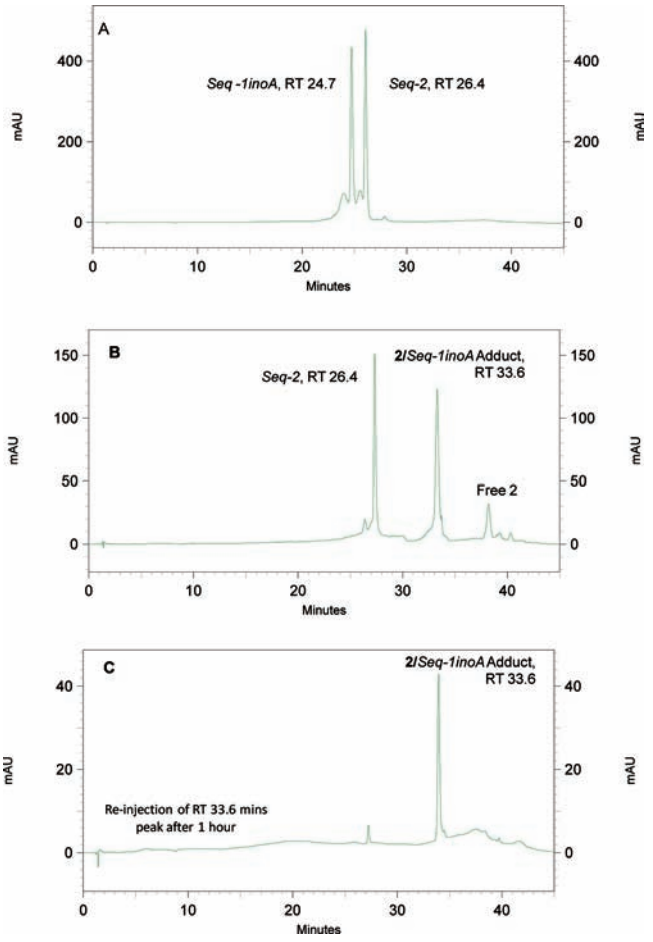

Figure 2. HPLC chromatograms: (A) *Seq-1inoA*/*Seq-2* duplex showing the denatured *Seq-1inoA* at RT 24.7 min and *Seq-2* at RT 26.4 min. (B) After incubating the *Seq-1inoA*/*Seq-2* duplex with **2** for 6 h showing the **2**/*Seq-1inoA* monoadduct at RT 33.6 min. (C) After reinjection of the **2**/*Seq-1inoA* adduct (collected from peak at RT 33.6 min in Figure 2B) after 1 h, demonstrating the stability of this single-stranded PBD/DNA monoadduct.

MALDI-TOF-MS (SI), proving that no change in mass had occurred either before or after injection onto the HPLC.

To obtain further evidence for the stability of the PBD/SS DNA adduct, another duplex was designed, *Seq-1inoB*/*Seq-2* (Duplex 3), in which guanine 5 had been mutated to a non-nucleophilic inosine in *Seq-1inoB* (*i.e.*, 5′-TATAIATGTATA-3′; Table 1) with *Seq-2* acting as the complementary strand. The resulting duplex, which also contained only one guanine residue, offered a kinetically favorable Py-G-Py binding site[13] for the PBD compared to the thermodynamically favored Pu-G-Pu motif[23] offered by Duplex 2. Analysis of the annealed Duplex 3 alone using identical HPLC conditions provided two peaks at RT 25.3 and 26.4 min, and their structures were confirmed by MALDI-TOF-MS as *Seq-1inoB* and *Seq-2*, respectively (Figure S2A, SI). After incubation of **2** with Duplex 3 for 6 h, the **2**/*Seq-1inoB* SS adduct peak was observed at RT 33.7 min. The adduct was collected and identified by MALDI-TOF-MS, and was then reinjected after 1 h onto the HPLC column. A major peak identified as the **2**/*Seq-1inoB* adduct was observed at 33.7 min with a minor peak at 25.3 min identified as *Seq-1inoB* (Figure S2B, SI). As a *Seq-1inoA* peak was not observed in the experiment

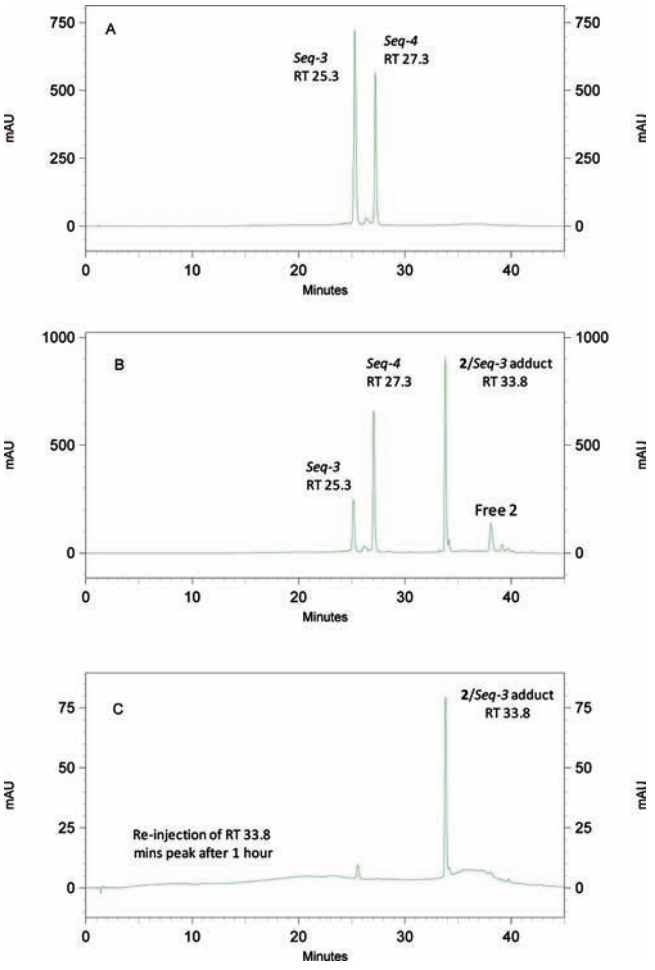

Figure 3. HPLC chromatograms: (A) *Seq-3*/*Seq-4* Duplex showing the denatured *Seq-3* and *Seq-4* at RT 25.3 min and RT 27.3 min, respectively. (B) After incubating the *Seq-3*/*Seq-4* Duplex with **2** for 3 h showing the **2**/*Seq-3* monoadduct at RT 33.8 min. (C) Chromatogram obtained after reinjection of the **2**/*Seq*-3 adduct (collected from peak at RT 33.8 min in Figure 3B) after 1 h, showing the stability of this single-stranded PBD/DNA monoadduct.

with Duplex 2 (Figure 2), this suggested that the **2**/*Seq-1inoB* SS adduct is relatively less stable than the **2**/*Seq-1inoA* adduct, perhaps reflecting their different sequences (*i.e.*, Py-G-Py vs Pu-G-Pu, respectively). The RT 33.7 min peak was subjected to MALDI-TOF-MS to reconfirm it as the 1:1 **2**/*Seq-1inoB* adduct. The stability of these SS DNA adducts was surprising given that SS oligonucleotides have no minor groove structure, and that literature reports suggest that loss of minor groove structure results in detachment of PBDs from the DNA duplex.[45] As control experiments, **2** was incubated with both *Seq-1inoA* and *Seq-1inoB* independently for at least 72 h, but no adduct formation was observed either by HPLC or MALDI-TOF-MS. This confirmed previous literature reports that PBDs require minor groove structure within a duplex to covalently bond to DNA.[38]

We have previously shown that PBDs can form stable adducts with hairpin-forming single-stranded 17-mer oligonucleotides.[38] Both *Seq-1inoA* and *Seq-1inoB* have the potential to form mismatched hairpins due to the presence of palindromic TATA sequences at both their 5́- and 3́-ends. As there was a possibility that both the **2**/*Seq1inoA* and **2**/*Seq1inoB* adducts collected from

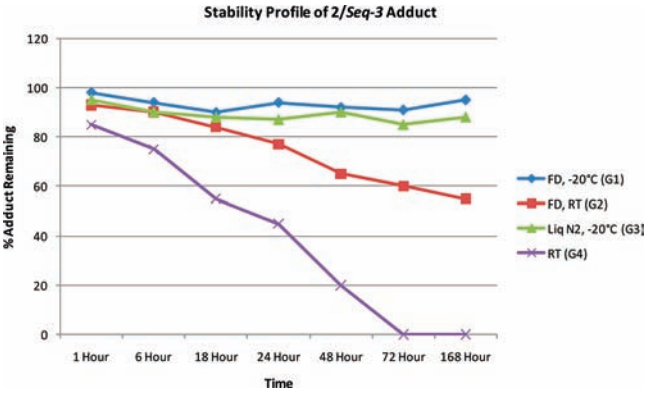

Figure 4. Stability of the **2**/Seq-3 single-stranded PBD/DNA monoadduct after storage under four different conditions: Group 1 (**G1**), freeze-dried (FD) and kept at −20 °C. Group 2 (**G2**), freeze-dried and stored at RT. Group 3 (**G3**), immediately frozen in liquid nitrogen after collection and stored at −20 °C. Group 4 (**G4**), stored in solution in HPLC eluent at room temperature without lyophilization or freezing.

the HPLC could form mismatched hairpin structures that might stabilize the adducts due to some minor groove structure, experiments were devised to exclude this possibility. Thus, *Seq-3*/*Seq-4* (containing a favorable Pu-G-Pu sequence; Duplex 4) and *Seq-5*/*Seq-6* (containing a less favored Py-G-Py sequence; Duplex 5) were designed, both of which offered only one guanine for covalent interaction with the PBD but without any terminal palindromic sequences that might encourage hairpin formation. Injection of annealed Duplex 4 (*Seq-3*/*Seq-4*) on to the HPLC column provided two distinct peaks at RT 25.3 and 27.3 min (Figure 3A) identified as *Seq-3* and *Seq-4*, respectively, by MALDI-TOF-MS. Incubation of Duplex 4 with **2** for 3 h led to a chromatographic profile similar to that obtained with *Seq-1inoA*/*Seq-2* (Duplex 2) (Figure 3B). The **2**/*Seq-3* monoadduct was observed at RT 33.8 min and then isolated, and its identity confirmed by MALDI-TOF-MS. Reinjection after 1 h produced an identical peak (both by RT and MS, SI), thus establishing its relative stability (Figure 3C). Similarly, incubating the annealed Duplex 5 with **2** for 6 h provided the **2**/*Seq-5* monoadduct at RT 34.1 min (Figure S3B, SI), which was isolated and its identity confirmed. This adduct contained the less thermodynamically favored Py-G-Py sequence and so was less stable (Figure S3C, SI) than the **2**/*Seq3* adduct that was based on a Pu-G-Pu sequence (Figure 3C). This second set of experiments with *Seq-3*/*Seq-4* and *Seq-5*/*Seq-6* ruled out hairpin formation and confirmed literature reports that a Pu-G-Pu sequence represents a more thermodynamically preferred binding site than Py-G-Py,[13] which is kinetically preferred (*i.e.*, **2**/*Seq-1inoA* and **2**/*Seq-3* adducts were both more stable than the **2**/*Seq-1inoB* and **2**/*Seq-5* adducts).

Next, the **2**/*Seq-3* monoadduct was selected for a stability study as it cannot form hairpin structures and contains the thermodynamically favored Pu-G-Pu binding motif. Approximately 28 fractions of the adduct were collected through repetitive injections of an incubation mixture onto the HPLC column. These fractions were pooled and mixed, and the resulting solution divided into four groups (**G1**−**G4**) containing seven aliquots each. **G1** and **G2** aliquots were freeze-dried and then stored at −20 °C or room temperature, respectively. **G3** aliquots were immediately frozen in liquid N_2 and then stored at −20 °C, while **G4** aliquots were stored in solution in HPLC eluent at room temperature without lyophilization or freezing.

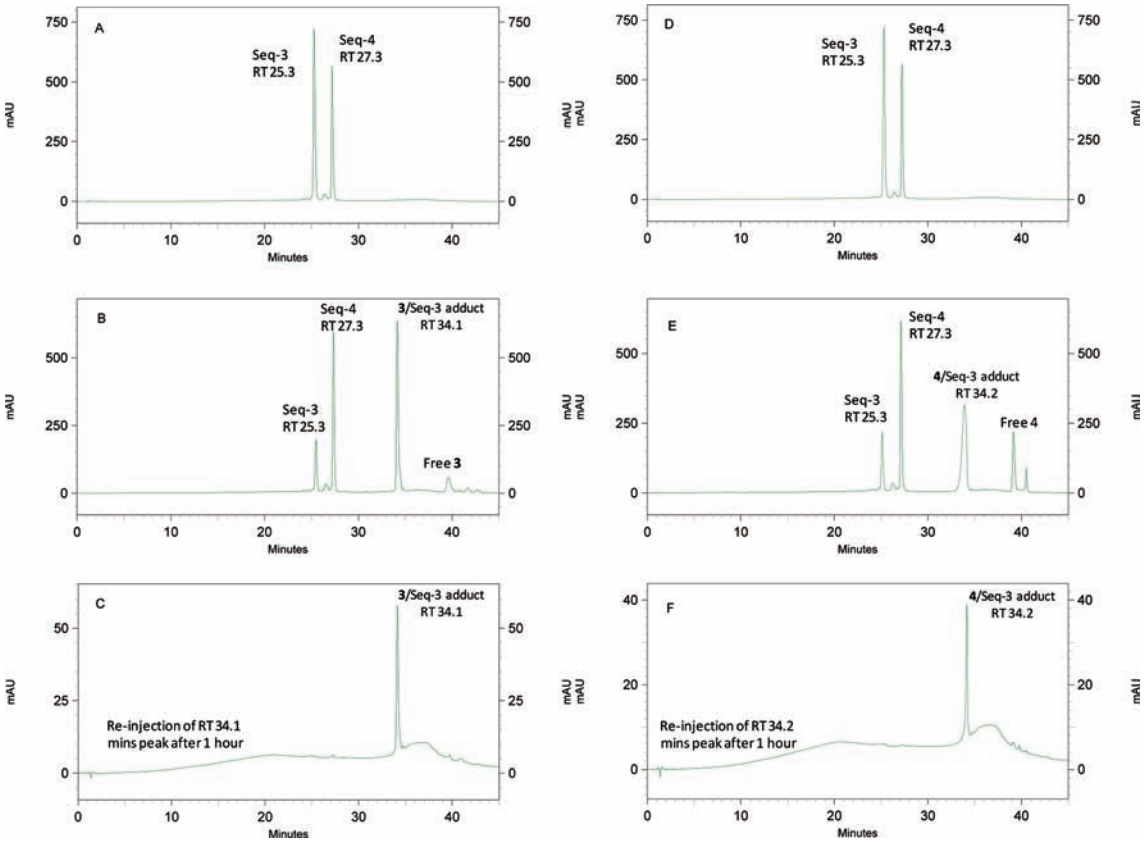

Figure 5. HPLC Chromatograms: (A and D) *Seq-3*/*Seq-4* Duplex showing the denatured *Seq-3* and *Seq-4* at RT 25.3 and 27.3 min, respectively. (B) After incubating the *Seq-3*/*Seq-4* Duplex with **3** for 3 h showing the **3**/*Seq-3* SS adduct at RT 34.1 min. (C) Chromatogram obtained after reinjection of the **3**/*Seq*-3 adduct (collected from peak at RT 34.1 min in Figure 5B) after 1 h, showing the stability of this single-stranded PBD/DNA SS adduct. (E) After incubating the *Seq-3*/*Seq-4* Duplex with **4** for 3 h showing the **4**/*Seq-3* SS adduct at RT 34.2 min; **F**, Chromatogram obtained after reinjection of the **4**/*Seq*-3 adduct (collected from peak at RT 34.2 min in Figure 5E) after 1 h, showing the stability of this SS PBD/DNA SS adduct.

Aliquots from each group were analyzed by HPLC after 1, 6, 18, 24, 48, 72, and 168 h (7 days). For each analysis, one of the aliquots was thawed (if required) and then injected onto the HPLC column (Figure 4). These data show that the SS DNA monoadduct remained stable over 7 days when lyophilized and stored at −20 °C (**G1**), although at room temperature degradation started after 18 h with approximately 60% remaining after 7 days (**G2**). Initial freezing of the adduct and storage at −20 °C also maintained stability for 7 days (**G3**). On the other hand, if left in solution at room temperature (**G4**), a rapid decline in concentration of the adduct occurred, with complete reversion to DNA and free drug after 72 h. In order to assess the effect of the organic component of the HPLC solvent (*i.e.*, acetonitrile) on the stability of adducts, the experiments were repeated but with freeze-drying of the collected fractions to remove solvent before redissolving in 100 mM ammonium acetate buffer. These samples were stored at room temperature and then analyzed at the same time points. After removal of acetonitrile, the **2**/*Seq-3* adduct showed a slightly greater stability, although complete degradation had occurred after storing at room temperature for 96 h (Figure S4, SI).

After observing the relative stability of the **2**/SS DNA adducts, the next goal was to establish whether a PBD dimer of different linker length and a PBD monomer would behave in a similar way. For this purpose we selected DRG-16 (SG-2057, **3**, Figure 1A), a PBD dimer with a longer pentyldioxy linker (C8−O−$(CH_2)_5$−O−C8′) that spans approximately seven base pairs in its entirety, and GWL-78 (**4**, Figure 1A), a PBD monomer with a C8-linked AT-preferring dipyrrole unit which spans approximately six base pairs. Incubation of **3** with Duplex 4 (*Seq-3*/*Seq-4*) for 3 h followed by injection onto the HPLC column resulted in the **3**/*Seq-3* monoadduct at RT 34.1 min (Figure 5B). As in previous experiments, the **3**/*Seq-3* monoadduct was collected and reinjected onto the HPLC column which provided a single peak at RT 34.1 min (Figure 5C), confirmed as the **3**/*Seq-3* monoadduct by MALDI-TOF-MS (Table 2). Similar incubation of PBD monomer **4** with Duplex 4 (*Seq-3*/*Seq-4*) for 3 h followed by HPLC analysis provided the **4**/*Seq-3* adduct peak at RT 34.2 min (Figure 5E). Collection and reinjection of the **4**/*Seq-3* adduct peak resulted in a single peak at RT 34.2 min (Figure 5F) confirmed as the **4**/*Seq-3* adduct by MALDI-TOF-MS. The relative stabilities of both the **3**/*Seq-3* and **4**/*Seq-3* adducts when stored in solution at room temperature or frozen at −20 °C were determined by a time course study in which the monoadducts were injected onto the HPLC column at various time intervals. The monoadducts appeared relatively stable (*i.e.*, >80% intact) after storing at −20 °C for 96 h, while after storing at room temperature only ∼60% adducts of the adducts remained after 18 h with complete disappearance after 72 h (Figure S5, SI). The overall stability profiles for the **3**/*Seq-3* and **4**/*Seq-3* SS DNA adducts were similar to those observed for the **2**/*Seq-3* adducts (*i.e.*, Figure 4). Together, these results suggest that the observed behaviour is universal, with single-stranded adducts of two PBD dimers (**2** and **3**) and one PBD monomer (**4**) remaining stable for at least 96 h at −20 °C, and 18 h at room temperature.

Table 2. Theoretical and Observed Masses of PBD/Oligonucleotide 1:1 Adducts

adduct	retention time (min)	theoretical PBD/SS DNA adduct mass (1:1)	observed PBD/SS DNA adduct mass (1:1)
2/(*Seq-1*/*Seq-1*) interstrand duplex adduct (Pu-GATC-Py)	28.7	7844.01	7841.30
2/*Seq-1inoA* monoadduct (Pu-GATI-Py)	33.6	4225.09	4222.99
2/*Seq-1inoB* monoadduct (Pu-IATG-Py)	33.7	4225.09	4225.14
2/*Seq-3* monoadduct (Pu-GATA-Py)	33.8	4224.11	4222.73
2/*Seq-5* monoadduct (Pu-TATG-Py)	34.1	4206.11	4201.82
2/(*Seq-3*/*Seq-11*) mismatched interstrand duplex adduct	27.8	7867.61	7877.00
3/ *Seq-3* monoadduct (Pu-GATA-Py)	34.1	4252.50	4251.00
4/ *Seq-3* monoadduct (Pu-GATA-Py)	34.2	4258.10	4254.70
2/*Seq-7* monoadduct	30.9	3293.50	3294.30
3/*Seq-7* monoadduct	31.5	3321.50	3316.70
4/*Seq-7* monoadduct	31.6	3329.30	3328.20
2/*Seq-9* monoadduct	31.4	5458.90	5458.10

The DNA duplexes used in the study up to this point were all 12-mers containing only one PBD binding site (*i.e.*, AGA or TGT). The number of guanines present in these duplexes was restricted to one to avoid multiple adduct formation leading to complex HPLC profiles that would be difficult to interpret. Next, to explore the effect of duplex length on the stability of SS DNA adducts, we designed 9-mer (Duplex 6) and 16-mer (Duplex 7) oligonucleotide duplexes (Table 1). The shorter Duplex 6 provided peaks at RT 19.0 and 20.4 min, and their identities were confirmed by MALDI-TOF-MS as *Seq-7* and *Seq-8*, respectively. Incubation of **2** with Duplex 6 provided a **2**/*Seq-7* SS adduct at RT 30.9 min (Figure S6, SI) which was collected and its identity confirmed by MALDI-TOF-MS. Similar HPLC studies with **3** and **4** provided **3**/*Seq-7* and **4**/*Seq-7* adducts at RT 31.5 and 31.6 min, respectively (Figures S7 and S8, SI), the identities of which were confirmed by MALDI-TOF-MS. The stabilities of the **2**/*Seq-7*, **3**/*Seq-7* and **4**/*Seq-7* adducts at room temperature and at −20 °C over 96 h were determined by injection of the adducts onto the HPLC column at various time intervals (Figure S9, SI). The stability profiles showed that all three adducts were significantly stable up to 18 h at room temperature or 96 h at −20 °C.

To observe the effect of lengthening the DNA sequence, **2** was incubated with the 16-mer Duplex 7 (*Seq-9*/*Seq-10*). Injecting the annealed duplex onto the HPLC column provided peaks at RT 21.4 and 23.5 min (Figure 6A) which were identified as *Seq-9* and *Seq-10*, respectively, by MALDI-TOF-MS. Injecting a 3-hour incubation mixture of **2** and Duplex 7 onto the HPLC column provided a **2**/*Seq-9* SS adduct at RT 31.4 min (Figure 6B). The adduct identity was confirmed by collection and reinjection (Figure 6C) followed by MALDI-TOF-MS. Next, the stability of the adduct under two different storage conditions (RT and −20 °C) was studied over 96 h through repetitive injection onto the HPLC column at various time points. When the stability profile of the **2**/*Seq-9* adduct (Figure S10, SI) was compared with those of the other SS DNA adducts (*i.e.*, Figures 4 and S9 [SI]), it was clear that for the 9- to 16-mer duplexes used in the study, the stability of the adducts was independent of duplex length. Although it is reasonable to assume that single-stranded PBD adducts may form in significantly longer stretches of genomic DNA in cells during enzymatic processes that separate duplex DNA (*e.g.*, transcription and replication), unfortunately the current HPLC/MS methodology is unable to analyze genomic DNA adducts.

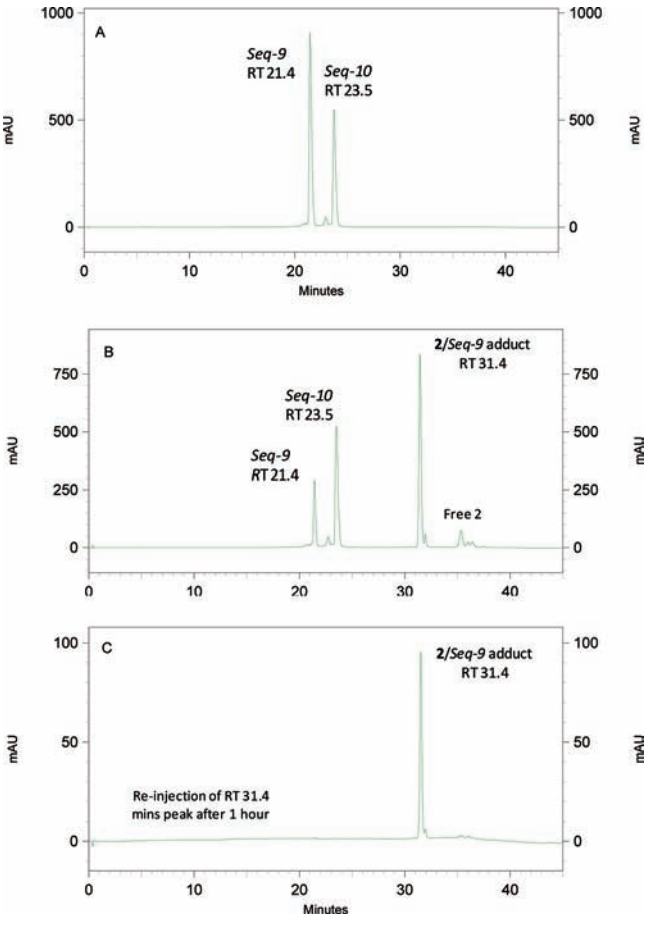

Figure 6. HPLC Chromatograms: (A) *Seq-9*/*Seq-10* duplex showing the denatured *Seq-9* and *Seq-10* at RT 21.4 and 23.5 min, respectively; (B) After incubating the *Seq-9*/*Seq-10* duplex with **2** for 3 h showing the **2**/*Seq-9* SS adduct at RT 31.4 min; (C) Chromatogram obtained after reinjection of the **2**/*Seq-9* adduct (collected from peak at RT 31.4 min in Figure 6B) after 1 h, showing the stability of this PBD/SS DNA adduct.

A further set of experiments was designed to establish whether a complementary single strand of DNA with a suitably placed guanine could be added to a single-stranded SJG-136 adduct to

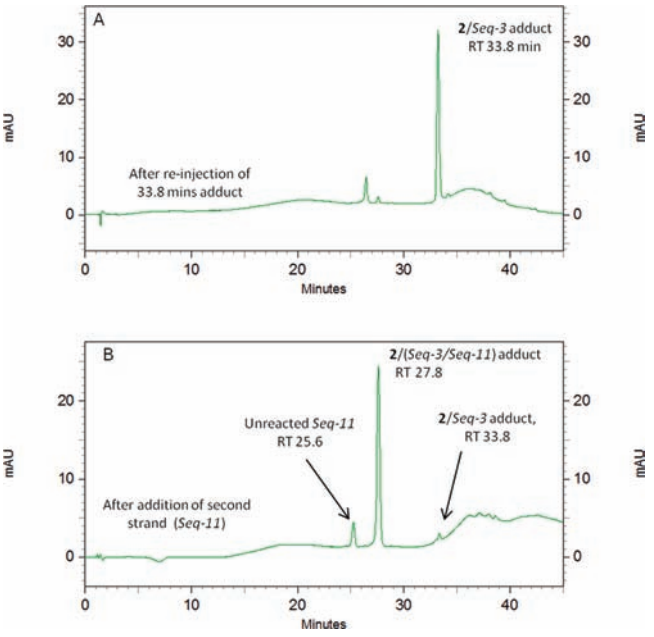

Figure 7. HPLC chromatograms: (A) **2**/*Seq-3* SS adduct obtained after incubating **2** with the *Seq-3*/*Seq-4* duplex, followed by collection of the peak at RT 33.8 min and reinjection. (B) Chromatogram obtained after addition of *Seq-11* to the lyophilized **2**/*Seq-3* SS adduct (obtained from Figure 7A) followed by heating to 45 °C for 5 min to form the interstrand cross-linked **2**/(*Seq-3*/*Seq-11*) adduct visible at RT 27.8 min.

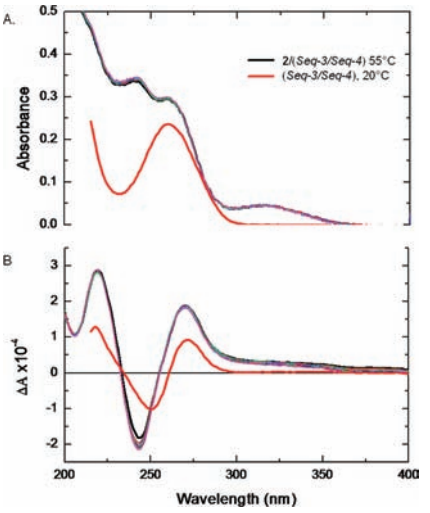

Figure 8. (A) UV and (B) CD spectra of the **2**/(*Seq-3*/*Seq-4*) adduct as a function of time at 55 °C. Heating at the melting point of the adduct ensured that the **2**/*Seq-3* PBD/DNA SS adduct (black line) was the active CD species throughout the heating procedure. The colored lines overlapping with the black line indicate CD spectra recorded at different time points at 55 °C over 2 h. The CD spectrum of the duplex alone is shown in red.

regenerate a duplex interstrand cross-linked adduct. For this purpose we selected the **2**/*Seq-3* adduct, and also designed a new sequence, 5′-ATATGATCTATA-3′ (*Seq-11*, Table 1), that could form a one-base mismatch duplex with *Seq-3* (5′- TATAGATAATAT-3′) thus re-forming an interstrand cross-linked adduct. The freeze-dried **2**/*Seq-3* adduct was reconstituted using 100 mM ammonium acetate buffer at pH 7.0 (Figure 7A), *Seq-11* added and the mixture heated briefly to 45 °C for 5 min followed by cooling to room temperature. Analysis of the reaction mixture (Figure 7B) revealed the emergence of a duplex **2**/(*Seq-3*/*Seq-11*) adduct at 27.8 min as the major peak, whereas no **2**/*Seq-11* adduct was observed. This result confirmed that the free imine functionality of **2** within the single-stranded **2**/*Seq-3* adduct could covalently bond to the nucleophilic guanine in the second strand (*Seq-11*) to produce an interstrand cross-linked adduct within the mismatched duplex. The brief heating to 45 °C helped to anneal the duplex, whereas heating to 70 °C (the usual temperature for annealing) was avoided as it could have detached the covalently bound **2** from *Seq-3*.

Comparative melting studies were also carried out on Duplexes 3 and 4 to confirm that covalent monoadducts had initially formed (Table S1, SI). The T_m values of the monoalkylated **2**/(Duplex 3) and **2**/(Duplex 4) adducts (45 and 57.5 °C, respectively) were consistently higher than for the duplexes alone (19 and 20 °C, respectively), confirming that stabilization through covalent ligand attachment had occurred. An estimate of the relative proportions of all species present throughout the temperature/time-course experiments was also calculated (Figure S11, SI).

Further experiments using circular dichroism (CD) spectroscopy were carried out to confirm the HPLC/MS-based observations. The CD spectra of the 12-mer duplexes (Duplexes 2−5) changed significantly upon addition of **2** in the same ratio as used in the HPLC experiments, thus confirming ligand binding (Figure S12, SI). It has been previously reported that PBDs such as **2** do not react with nonhairpin-forming single-stranded oligonucleotides and that no changes in CD signals are observed when PBDs are added to them.[38] Therefore, the enhancement of CD signals upon addition of **2** to the four oligonucleotide pairs (Figures S12A−D, SI) confirmed that these were in the duplex form prior to adduct formation. However, these duplexes have low melting temperatures as the oligonucleotides are relatively short, so there is most likely an equilibrium between duplex and single-stranded forms[8] at room temperature. As **2** is added to each solution, the equilibrium should shift toward the duplex species, as the latter are stabilized by adduct formation. The change in CD spectra for *Seq-1inoB*/*Seq-2* (Duplex 3) and *Seq-3*/*Seq-4* (Duplex 4) as they reacted with **2** was also monitored at different temperatures, and a gradual loss of the **2**-induced CD signal was observed at temperatures higher than 60 °C, with complete loss of signal by 80 °C at the point of detachment of **2** from the DNA (Figure S13, SI).

To further investigate the relative stability of a SS DNA monoadduct, **2**/(*Seq-3*/*Seq-4*) was subjected to a sustained heating experiment at 55 °C while recording both the UV and CD spectra throughout the experiment. Heating up to 55 °C separated the duplex leaving **2** covalently attached to the single strand (*i.e.*, guanine 5 of *Seq-3*). Controlled heating at 55 °C for 2 h showed that the CD spectrum remained significantly enhanced compared to the DNA alone throughout the experiment, confirming that **2** remained attached to the single-strand (Figure 8). This experiment clearly demonstrated the relative stability of the **2**/*Seq-3* monoadduct in the absence of minor groove structure. Also, it was interesting to observe that the shift in CD minimum for the *Seq-3*/*Seq-4* duplex after the addition of **2** (Figure S12, SI) was consistently observed when **2**/(*Seq-3*/*Seq-4*) was subjected to a sustained heating experiment at 55 °C (Figure 8B). The data for **2**/(*Seq-3*/*Seq-4*) in Figure 8A indicate that **2** contributes to the absorption, and thus also to the CD spectrum in the

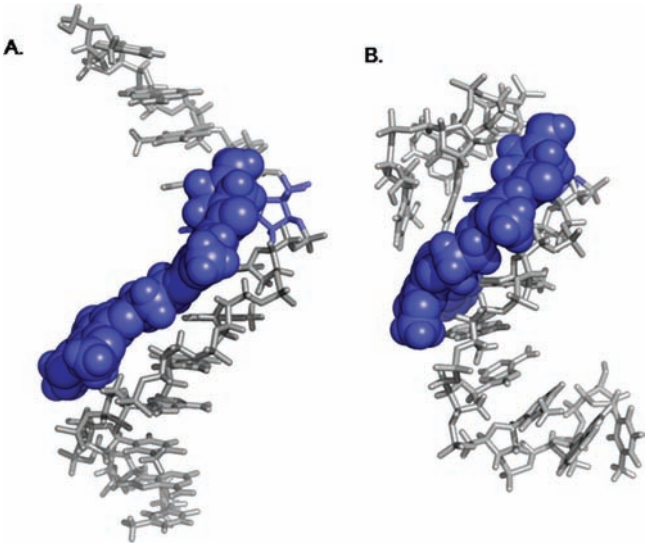

Figure 9. (A) Energy minimized model of the **2**/*Seq*-3 SS adduct at the start of the molecular dynamics simulation. (B) Last frame of the 2 ns molecular dynamics simulation showing the 5′-end of the DNA strand curling inward to make internal contacts with the ligand while the 3′-end remains in a state similar to its original conformation (see Supporting Information).

260−200 nM region. Therefore, any shift in the CD minimum in this wavelength range will consist of contributions from both **2** and the nucleic acid when it is still associated with **2**. This observation provided further proof that **2** remained covalently attached to the single-stranded DNA throughout the heating experiment.

Finally, molecular dynamics simulations were carried out to model the behavior of **2** when covalently bound to a single strand of DNA (*Seq*-3), to explore why such a PBD/DNA adduct can remain stable despite a loss of minor groove structure (Figure 9A,B). Two essential observations were made from a simulation carried out over 2 ns (Figure 9B). First, **2** itself remained in an elongated conformation and adhered to the remaining single strand of DNA through van der Waals interactions and a hydrogen bond between the N10−H of the PBD and the lone pair of electrons of the N3 atom of adenine-6. Second, the region of DNA in which **2** was in direct contact (*i.e.*, adenine 4 to adenine 9) underwent relatively little conformational variation compared to the free ends of the DNA which were highly flexible (see rms graph in Figure S14, SI). Over the time scale of the simulation, the 5′-end of the single DNA strand curled inward and made internal contacts with the ligand, while the 3′-end remained in a state similar to its original conformation. This may be due to differences in initial orientation of the bases with respect to the ligand at the 5′-end of the single strand compared to those at the 3′-end (see Dynamics Movie in SI).

■ CONCLUSION

In conclusion, we have observed and isolated for the first time, stable single-stranded PBD/DNA adducts of both PBD monomers and dimers, verified using two independent techniques (HPLC/MS and CD spectroscopy). This observation is surprising given that PBDs are well-known to require DNA minor-groove structure for adduct formation. Although we have found that single-stranded PBD/DNA adducts result only from dissociation of double-stranded adducts, it is reasonable to assume that single-stranded PBD adducts may form in genomic DNA in cells during enzymatic processes known to separate the two strands (*e.g.*, transcription and replication). Therefore, this observation could impact on understanding the mechanism of action of PBD agents in both cellular and *in vivo* systems. Furthermore, it may be relevant to understanding how PBD/DNA adducts are repaired in cells, and how this relates to the development of resistance. The observation may also lead to a re-evaluation of previously published biophysical, biochemical, and biological experiments on PBD molecules in which the observed activity was assumed to be due to double-stranded DNA adducts only. It could also influence the choice of pharmacodynamic end-point assays used in future clinical trials of PBD agents.

■ MATERIALS AND METHODS

HPLC/MS Assay. *Single-Stranded Oligonucleotides.* The single-stranded (SS) oligonucleotides were purchased from Eurogentec Ltd. (UK) and AtdBio Ltd. (Southampton, UK) in lyophilized form.

Double-Stranded Oligonucleotides. Each oligonucleotide was dissolved in 100 mM ammonium acetate (Sigma-Aldrich, UK) to form a stock solution of 2 mM which was later diluted to 1 mM by addition of annealing buffer (10 mM Tris/50 mM sodium chloride/1 mM EDTA). Solutions of double-stranded DNAs were prepared by heating the complementary SS oligonucleotides (1 mM) in annealing buffer (pH 8.5) to 70 °C for 10 min in a heating/cooling block (Grant Bio, UK). The solutions were then allowed to cool slowly to room temperature followed by storage at −20 °C overnight to ensure completion of the annealing process. Working solutions of DNA duplexes of 50 μM were prepared by diluting the stored solutions with 20 mM ammonium acetate.

*PBD Dimer SJG-136 (**2**).* The PBD dimer **2** was supplied by Ipsen Ltd. (Batch Number: SG2000.003) and was dissolved in 50:50 v/v methanol/water to form a stock solution of 3 mM which was stored at −20 °C for no longer than four months. Working solutions of 200 μM were prepared by diluting the stock solution with nuclease free water. These were stored at −20 °C for not more than one week and thawed to room temperature for use when required.

*PBD Dimer DRG-16 (**3**).* The PBD dimer **3** was supplied by Spirogen Ltd. (Batch Number: SG2057.002) and was dissolved in 50:50 v/v methanol/water to form a stock solution of 3 mM which was stored at −20 °C for no longer than four months. Working solutions of 200 μM were prepared by diluting the stock solution with nuclease-free water. These were stored at −20 °C for not more than one week and thawed to room temperature for use when required.

*PBD Monomer GWL-78 (**4**).* The PBD monomer **4** was provided by Spirogen Ltd. (Batch No. SG2274.005) and was dissolved in DMSO to form a stock solution of 10 mM which was stored at −20 °C for no longer than four months. Working solutions of the drug of 200 μM were prepared by diluting the stock solution with 100 mM ammonium acetate solution. These were stored at −20 °C for no longer than one week, and thawed to room temperature for use when required.

Preparation of PBD/DNA Complexes. PBD/DNA complexes were prepared by adding a working solution of **2**, **3** or **4** to a duplex oligonucleotide solution in a 4:1 molar ratio at room temperature. This incubation mixture was then agitated for 5−10 s using a vortex mixer.

Ion-Pair Reversed-Phase HPLC. Analysis was performed on a Thermo Electron HPLC system equipped with a 4.6 × 50 mm Xterra MS C18 column packed with 2.5 μM particles (Waters Ltd., UK), a UV 1000 detector, an AS3000 autosampler, a SCM1000 vacuum degasser and Chromquest software (Version 4.1), and also on a Waters e2695 separation module fitted with a Waters 2489 UV detector with a 2.1 mm × 50 mm Xbridge OST C18 column packed with 2.5 μM particles (Waters Ltd., UK).

A gradient system of 100 mM triethyl ammonium bicarbonate (TEAB) as buffer A and 40% acetonitrile in water (HPLC grade, Fischer Scientific, UK) as buffer B was used. For buffer A, a 1 M preformulated solution of TEAB was purchased from Sigma-Aldrich (UK) and diluted to the required concentration with HPLC-grade water (Fischer Scientific, UK). The gradient was ramped from 90% A at 0 min to 50% at 20 min, then 35% at 30 min and finally to 10% at 45 min. UV absorbance was monitored at 254 nm, and fractions containing separated components were collected manually, combined when appropriate, lyophilized, and then analyzed using MALDI-TOF-MS.

Lyophilization of HPLC Fractions. Single or combined HPLC fractions were lyophilized using two different methods depending on the final volume. For smaller volumes (less than 0.5 mL), lyophilizations were carried out in a SpeedVac (Thermo Electron) using a temperature-free 4 h program. For larger volumes, the solvent was initially frozen in a glass vial using liquid nitrogen, and then freeze-dried (Heto Lyolab 3000) for 2−6 h.

Mass Spectrometric Analysis. *MALDI-TOF.* An Applied Biosystems Voyager DE-Pro Biospectrometry Workstation Matrix-Assisted Laser Desorption/Ionization Time of Flight (MALDI-TOF) mass spectrometer (Framingham, MA, U.S.A.) was used to obtain MALDI-TOF spectra of components within lyophilized fractions. Samples from fractions containing single components were prepared by diluting with matrix (37 mg of 2′,4′,6′-trihydroxyacetophenone monohydrate [THAP] in 1 mL of ACN, 45 mg of ammonium citrate in 1 mL of water - mixed 1:1) either 2:1, 1:1, or 1:5 (sample/matrix) prior to MALDI-TOF analysis. One microliter of sample was spotted onto the MALDI target plate and allowed to dry. Samples were then analyzed in positive linear mode using delayed extraction (500 ns) and an accelerating voltage of 25000 V. Acquisition was between 4000−15000 Da with 100 shots/spectrum.

Circular Dichroism and Thermal Denaturation Studies. The UV and CD spectra of the oligonucleotides and PBD/oligonucleotide complexes were acquired on a Chirascan-Plus spectrometer (Applied Photophysics Ltd., Leatherhead, UK). The UV absorbance and CD spectra were measured between 200 and 500 nm in a strain-free rectangular 5 or 10 mm cell. The instrument was flushed continuously with pure evaporated nitrogen throughout the measurements. Spectra were recorded using a 1 nm step size, a 1s time-per-point, and a spectral bandwidth of 1 or 2 nm. Addition of a PBD to the oligonucleotide solutions was carried out while maintaining a constant concentration of DNA. All spectra were acquired at room temperature and the buffer baseline corrected. All CD spectra were smoothed using the Savitsky-Golay method, and a window factor of 4−12 was used for better presentation.

The *Dynamic Multi-Mode Spectroscopy (DMS)* technology provided by Applied Photophysics Ltd. was employed for the thermal measurements. The CD spectra were first recorded at room temperature (20 °C), then again after cooling to 6 °C, heating to the highest temperature (94 °C), recooling to 6 °C and heating back to 20 °C. The melting profiles monitored at a particular wavelength were recorded during both the heating and cooling phases. The instrument was equipped with a Quantum (NorthWest, USA) TC125 Peltier unit set to change temperature from 6 → 94 °C at a rate of 1 °C/min with a 2 °C step-size. The same parameters were set for the cooling process (94 → 6 °C). A 2 s time per points CD measurement time scale was employed in the 400−215 nm region with a 2 nm spectral bandwidth. Temperature was measured directly using a thermocouple probe inserted in the solutions. Melting temperatures were determined from derivative spectra produced in the Global Analysis T-Ramp software (Applied Photophysics Ltd.).

Molecular Modeling. In order to examine the structural feasibility of the various single-stranded monoalkylated PBD adducts, molecular models were constructed. To test the integrity of the structures under energetic conditions, dynamics simulations were carried out at room temperature (300 K). For example, minimized structures of SJG-136 (**2**) were constructed with ChemBioOffice (Cambridgesoft, Version 2010) and exported in PDB format. Missing residue and chain records were added, and atom names were made unique. The AMBER package[48] was used for subsequent conversion of files to the 'mol2' format applying Gasteiger charges (antechamber), with missing parameters added through the 'parmchk' routine. The DNA duplexes were made with AMBER, and the adducts constructed manually in the first instance using 'Xleap' while maintaining the S-configuration at the C11-position of covalent attachment of individual PBD units. Structures were then exported for minimization, initially restraining the DNA atoms to allow the bound ligand to find an optimal conformation within the minor groove without distorting the overall DNA structure. Subsequent minimization steps were applied while reducing the level of restraints on the DNA until all were eventually removed. The generalized Born/surface area (GB/SA) implicit solvent model was used with monovalent electrostatic ion screening simulated with the SALTCON parameter set to 0.2 (M) and with a long-range nonbonded cutoff employed.

Subsequent dynamics simulations over 2 ns were then performed under similar solvent conditions. With application of the SHAKE algorithm to C−H bond vibrations, a time step of 2 fs was used. Individual energy terms were saved every 200 steps (every 0.4 ps), and the recorded energies were used to plot graphs of the total potential energy of the constructs against the simulation time. The average potential energy for the whole simulation was also recorded. Conformational variation during the course of the dynamics simulations was examined by performing a rigid body rms fit for the atoms of each frame of the simulation compared to the first frame, followed by plotting this parameter against simulation time.

■ ASSOCIATED CONTENT

Supporting Information. HPLC traces, MS data, CD spectra, molecular models, MD simulation movie, and complete ref 48. This material is available free of charge via the Internet at http://pubs.acs.org.

■ AUTHOR INFORMATION

Corresponding Author
david.thurston@pharmacy.ac.uk

■ ACKNOWLEDGMENT

Applied Photophysics Ltd. (Surrey, UK) is thanked for providing a Chirascan instrument, and the Wellcome Foundation is acknowledged for supporting the KCL Biomolecular Spectroscopy Centre. Ipsen Ltd. and Spirogen Ltd. are thanked for providing samples of SJG-136 (**2**), and DRG-16 (**3**) and GWL-78 (**4**), respectively.

■ REFERENCES

(1) Cipolla, L.; Araujo, A. C.; Airoldi, C.; Bini, D. *Anti-Cancer Agents Med. Chem.* **2009**, *9*, 1.
(2) Thurston, D. E.; Bose, D. S. *Chem. Rev.* **1994**, *94*, 433.
(3) Antonow, D.; Thurston, D. E. *Chem. Rev.* **2011**, *111*, 2815.
(4) Thurston, D. E. In *Molecular Aspects of Anticancer Drug-DNA Interactions*; Neidle, S., Waring, M. J., Eds.; The Macmillan Press Ltd.: London, 1993; Vol. 1, p 54.
(5) Kamal, A.; Rao, M. V.; Laxman, N.; Ramesh, G.; Reddy, G. S. K. *Curr. Med. Chem.—Anti-Cancer Agents* **2002**, *2*, 215.

(6) Gregson, S. J.; Howard, P. W.; Hartley, J. A.; Brooks, N. A.; Adams, L. J.; Jenkins, T. C.; Kelland, L. R.; Thurston, D. E. *J. Med. Chem.* **2001**, *44*, 737.
(7) Gregson, S. J.; Howard, P. W.; Gullick, D. R.; Hamaguchi, A.; Corcoran, K. E.; Brooks, N. A.; Hartley, J. A.; Jenkins, T. C.; Patel, S.; Guille, M. J.; Thurston, D. E. *J. Med. Chem.* **2004**, *47*, 1161.
(8) Rahman, K. M.; Thompson, A. S.; James, C. H.; Narayanaswamy, M.; Thurston, D. E. *J. Am. Chem. Soc.* **2009**, *131*, 13756.
(9) Janjigian, Y. Y.; Lee, W.; Kris, M. G.; Miller, V. A.; Krug, L. M.; Azzoli, C. G.; Senturk, E.; Calcutt, M. W.; Rizvi, N. A. *Cancer Chemother. Pharmacol.* **2010**, *65*, 833.
(10) Narendran, A.; Jayanthan, A.; Singh, A.; Incoronato, A.; Desai, S.; Whitlock, J. *Pediatr. Blood Cancer* **2010**, *54*, 814.
(11) Hochhauser, D.; Meyer, T.; Spanswick, V. J.; Wu, J.; Clingen, P. H.; Loadman, P. M.; Cobb, M.; Gumbrell, L.; Begent, R. H. J.; Hartley, J. A.; Jodrell, D. I. *Clin. Cancer Res.* **2009**, *15*, 2140.
(12) Thurston, D. E. *Chemistry and Pharmacology of Anticancer Drugs*; CRC Press (Taylor & Francis): Boca Raton, FL, 2006; Vol. 1, p281.
(13) Rahman, K. M.; Vassoler, H.; James, C. H.; Thurston, D. E. *ACS Med. Chem. Lett.* **2010**, *1*, 427.
(14) Kamal, A.; Balakishan, G.; Ramakrishna, G.; Shaik, T. B.; Sreekanth, K.; Balakrishna, M.; Rajender; Dastagiri, D.; Kalivendi, S. V. *Eur. J. Med. Chem.* **2010**, *45*, 3870.
(15) Kamal, A.; Bharathi, E. V.; Ramaiah, M. J.; Dastagiri, D.; Reddy, J. S.; Viswanath, A.; Sultana, F.; Pushpavalli, S.; Pal-Bhadra, M.; Srivastava, H. K.; Sastry, G. N.; Juvekar, A.; Sen, S.; Zingde, S. *Bioorg. Med. Chem.* **2010**, *18*, 526.
(16) Kamal, A.; Devaiah, V.; Reddy, K. L.; Kumar, M. S. *Bioorg. Med. Chem.* **2005**, *13*, 2021.
(17) Kamal, A.; Khan, M. N. A.; Srikanth, Y. V. V.; Reddy, K. S.; Juvekar, A.; Sen, S.; Kurian, N.; Zingde, S. *Bioorg. Med. Chem.* **2008**, *16*, 7804.
(18) Baraldi, P. G.; Balboni, G.; Cacciari, B.; Guiotto, A.; Manfredini, S.; Romagnoli, R.; Spalluto, G.; Thurston, D. E.; Howard, P. W.; Bianchi, N.; Rutigliano, C.; Mischiati, C.; Gambari, R. *J. Med. Chem.* **1999**, *42*, 5131.
(19) Wells, G.; Martin, C. R. H.; Howard, P. W.; Sands, Z. A.; Laughton, C. A.; Tiberghien, A.; Woo, C. K.; Masterson, L. A.; Stephenson, M. J.; Hartley, J. A.; Jenkins, T. C.; Shnyder, S. D.; Loadman, P. M.; Waring, M. J.; Thurston, D. E. *J. Med. Chem.* **2006**, *49*, 5442.
(20) Brucoli, F.; Hawkins, R. M.; James, C. H.; Wells, G.; Jenkins, T. C.; Ellis, T.; Hartley, J. A.; Howard, P. W.; Thurston, D. E. *Bioorg. Med. Chem. Lett.* **2011**, *21*, 3780.
(21) Kamal, A.; Rajender; Reddy, D. R.; Reddy, M. K.; Balakishan, G.; Shaik, T. B.; Chourasia, M.; Sastry, G. N. *Bioorg. Med. Chem.* **2009**, *17*, 1557.
(22) Puvvada, M. S.; Hartley, J. A.; Jenkins, T. C.; Thurston, D. E. *Nucleic Acids Res.* **1993**, *21*, 3671.
(23) Puvvada, M. S.; Forrow, S. A.; Hartley, J. A.; Stephenson, P.; Gibson, I.; Jenkins, T. C.; Thurston, D. E. *Biochemistry* **1997**, *36*, 2478.
(24) Kotecha, M.; Kluza, J.; Wells, G.; O'Hare, C. C.; Forni, C.; Mantovani, R.; Howard, P. W.; Morris, P.; Thurston, D. E.; Hartley, J. A.; Hochhauser, D. *Mol. Cancer Ther.* **2008**, *7*, 1319.
(25) Hu, W.-P.; Tsai, F.-Y.; Yu, H.-S.; Sung, P.-J.; Chang, L.-S.; Wang, J.-J. *Chem. Res. Toxicol.* **2008**, *21*, 1330.
(26) Hsieh, M.-C.; Hu, W.-P.; Yu, H.-S.; Wu, W.-C.; Chang, L.-S.; Kao, Y.-H.; Wang, J.-J. *Toxicol. Appl. Pharmacol.* **2011**, *255*, 150.
(27) Osada, H.; Uramoto, M.; Uzawa, J.; Kajikawa, K.; Isono, K. *Agric. Biol. Chem.* **1990**, *54*, 2883.
(28) Hadjivassileva, T.; Thurston, D. E.; Taylor, P. W. *J. Antimicrob. Chemother.* **2005**, *56*, 513.
(29) Fotso, S. *Mini-Reviews Org. Chem.* **2010**, *7*, 68.
(30) Fotso, S.; Zabriskie, T. M.; Proteau, P. J.; Flatt, P. M.; Santosa, D. A.; Sulastri; Mahmud, T. *J. Nat. Prod.* **2009**, *72*, 690.
(31) Antonow, D.; Barata, T.; Jenkins, T. C.; Parkinson, G. N.; Howard, P. W.; Thurston, D. E.; Zloh, M. *Biochemistry* **2008**, *47*, 11818.
(32) Jenkins, T. C.; Hurley, L. H.; Neidle, S.; Thurston, D. E. *J. Med. Chem.* **1994**, *37*, 4529.
(33) Hopton, S. R.; Thompson, A. S. *Biochemistry* **2011**, *50*, 4720.
(34) Reddy, B. S. P.; Sharma, S. K.; Lown, J. W. *Curr. Med. Chem.* **2001**, *8*, 475.
(35) Smellie, M.; Bose, D. S.; Thompson, A. S.; Jenkins, T. C.; Hartley, J. A.; Thurston, D. E. *Biochemistry* **2003**, *42*, 8232.
(36) Rahman, K. M.; James, C. H.; Thurston, D. E. *Nucleic Acids Res.* **2011**, *39*, 5800.
(37) Rahman, K. M.; James, C. H.; Thurston, D. E. *Org. Biomol. Chem.* **2011**, *9*, 1632.
(38) Rahman, K. M.; Mussa, V.; Narayanaswamy, M.; James, C. H.; Howard, P. W.; Thurston, D. E. *Chem. Commun.* **2009**, 227.
(39) Sulc, M.; Fadrhoncova, I.; Jelinkova, M.; Chudomelova, M.; Felsberg, J.; Olsovska, J. *J. Chromatogr., Sect. A* **2011**, *1218*, 83.
(40) Kagan, M.; Chlenov, M.; Melnikov, S.; McConnell, O.; Bach, A. C.; Carter, G.; Failli, A.; Caggiano, T. J.; Shumsky, J. S.; Lubda, D. *J. Comb. Chem.* **2009**, *11*, 704.
(41) Narayanaswamy, M.; Griffiths, W. J.; Howard, P. W.; Thurston, D. E. *Anal. Biochem.* **2008**, *374*, 173.
(42) Martin, C.; Ellis, T.; McGurk, C. J.; Jenkins, T. C.; Hartley, J. A.; Waring, M. J.; Thurston, D. E. *Biochemistry* **2005**, *44*, 4135.
(43) Andreassen, P. R.; Ren, K. Q. *Curr. Cancer Drug Targets* **2009**, *9*, 101.
(44) Hartley, J. A.; Hamaguchi, A.; Suggitt, M.; Gregson, S. J.; Thurston, D. E.; Howard, P. W. *Invest. New Drugs* **2011**, *10*, 1007/s10637.
(45) Hurley, L. H.; Allen, C. S.; Feola, J. M.; Lubawy, W. C. *Cancer Res.* **1979**, *39*, 3134.
(46) Clingen, P. H.; Wu, J. Y. H.; Miller, J.; Mistry, N.; Chin, F.; Wynne, P.; Prise, K. M.; Hartley, J. A. *Biochem. Pharmacol.* **2008**, *76*, 19.
(47) Hartley, J. M.; Spanswick, V. J.; Hartley, J. A. *Methods Mol. Biol. (Clifton, N.J.)* **2011**, *731*, 309.
(48) Case, D. A.; et al. *Amber*; University of California: San Francisco, 2006.